ARTICLE
Journal of Cellular Biochemistry 112:1612–1621 (2011)

Journal of Cellular Biochemistry

The Mouse Mismatch Repair Protein, MSH3, is a Nucleoplasmic Protein that Aggregates into Denser Nuclear Bodies Under Conditions of Stress

Ian Holt,[1,2*] Le Thanh Lam,[1,2] Stéphanie Tomé,[3] Derick G Wansink,[4] Hein te Riele,[5] Geneviève Gourdon,[3] and Glenn E Morris[1,2]

[1] *Wolfson Centre for Inherited Neuromuscular Disease, RJAH Orthopaedic Hospital, Oswestry, Shropshire, SY10 7AG. UK*

[2] *Institute for Science and Technology in Medicine, Keele University, Keele, Staffordshire, ST5 5BG. UK*

[3] *INSERM, U781, Université Paris Descartes, Hôpital Necker Enfants Malades, 75015 Paris. France*

[4] *Department of Cell Biology, Radboud University Nijmegen Medical Centre, Nijmegen Centre for Molecular Life Sciences, 6525 GA Nijmegen. The Netherlands*

[5] *The Netherlands Cancer Institute, Antoni van Leeuwenhoek Hospital, Division of Molecular Biology, Plesmanlaan 121, 1066 CX Amsterdam. The Netherlands*

ABSTRACT

The mismatch repair protein, MSH3, together with MSH2, forms the MutSβ heterodimer which recognizes and repairs base pair mismatches and larger insertion/deletion loops in DNA. Lack of specific antibodies against mouse MSH3 has hampered studies of its expression and localization. Mouse MSH3 is not immunogenic in normal mice. This problem was overcome by immunizing *msh3*-knockout mice and generating a panel of ten monoclonal antibodies, two of which localize MSH3 specifically in cultured mouse cells and bind to an epitope containing amino-acids 33–37. The panel also includes two antibodies that recognise both mouse and human MSH3 and bind to a conserved epitope containing amino-acids 187–194. The mouse MSH3-specific antibodies show that MSH3 is a nuclear protein with a finely-granular nucleoplasmic distribution, largely absent from areas of condensed heterochromatin. Specificity of the localization was demonstrated by absence of immunostaining in a cell line from the *msh3*-knockout mouse. Furthermore, we show for the first time that stress treatment of mouse cells with ethanol or hydrogen peroxide caused the re-distribution of MSH3 into nuclear bodies containing the proliferating cell nuclear antigen (PCNA), a known binding partner of MutSβ. J. Cell. Biochem. 112: 1612–1621, 2011.

KEY WORDS: MISMATCH REPAIR; MSH3; MONOCLONAL ANTIBODIES; KNOCKOUT MOUSE; MYOTONIC DYSTROPHY; MUTSβ

The DNA mismatch repair (MMR) system is crucial in the maintaining of genome integrity in organisms. In eukaryotes, mismatch repair protein heterodimers, MutSα (MSH2-MSH6) and MutSβ (MSH2-MSH3), are involved in the initiation of repair of base-base mismatches and insertion/deletion loops. MutSα mainly binds base-base mismatches and small insertion/deletion loops whereas MutSβpredominantly processes larger insertion/deletion loops [reviewed in Jiricny, 2006]. These complexes are also involved in DNA damage signalling and have been implicated in repair of DNA interstrand crosslinks [Stojic et al., 2004; Hong et al., 2008; Zhao et al., 2009]. The MMR status determines the sensitivity of cells to H_2O_2, suggesting that MMR and/or MMR protein complexes may be involved directly in oxidative DNA damage responses. Other proteins involved in MMR are MutLα (MLH1-PMS2), MutLβ (MLH1-MLH3), proliferating cell nuclear antigen (PCNA). Exonuclease I and DNA ligase complete the DNA repair [Jiricny, 2006]. PCNA binds MutSα and MutSβ via a PIP box located in MSH3 and MSH6. PCNA and MutLα interact independently with MutSα, but they are in competition for binding MutSβ[Clark et al., 2000]. Inherited mutations in the MMR genes such as *MSH2, MSH6, MLH1* and *PMS2* underlie the cancer syndrome, hereditary nonpolyposis colorectal cancer (HNPCC, Lynch syndrome), and epigenetic silencing of *MSH2* and *MLH1* has been found in sporadic colorectal carcinomas (CRCs). MMR-defective tumours are characterized by microsatellite instability. MSH3 deficiency causes a weak mutator phenotype and no cancer

*Correspondence to: Dr. Ian Holt, E-mail: ian.holt@rjah.nhs.uk
Received 28 October 2010; Accepted 8 February 2011 • DOI 10.1002/jcb.23075 • © 2011 Wiley-Liss, Inc.
Published online 22 February 2011 in Wiley Online Library (wileyonlinelibrary.com).

predisposition, although it has been proposed as a risk factor in some sporadic cancers [Plaschke et al., 2004; Hirata et al., 2008]. The mechanisms of tumorigenesis have been studied *in vivo* including MMR deficient mouse models [Chao and Lipkin, 2006]. Recently, MMR and especially Mutsβ has been recognized as a major player in trinucleotide repeat instability [Pearson et al., 2005]. Several analyses have shown that MutSβ is involved in the formation of triplet repeat expansions across generations and in tissues from transgenic mouse models [Manley et al., 1999; van den Broek et al., 2002; Savouret et al., 2003; Wheeler et al., 2003; Owen et al., 2005; Foiry et al., 2006; Dragileva et al., 2009]. Moreover, MSH3 protein appears to be a limiting factor in the process of trinucleotide repeat expansions suggesting that triplet instability depends on MSH3 protein levels in germinal and somatic tissues from transgenic mice [Foiry et al., 2006; Dragileva et al., 2009]. MSH3 is a potential therapeutic target to prevent expansions in nucleotide repeat diseases such as myotonic dystrophy, since its ablation can prevent somatic and intergenerational repeat expansions, while producing little, if any, increase in cancer-related mutation rates, unlike MSH2 ablation [de Wind et al., 1999]. However, studies of endogenous MSH3 protein in transgenic mice have been hampered by lack of a specific antibody. Most commercially available MSH3 antibodies give strong non-specific signals in western blot and immunofluorescence experiments using tissues from Msh3-deficient mice as control. This is partly because MSH3 is highly-conserved and poorly immunogenic and partly because it is present at low levels in cells, relative to potential cross-reacting proteins. We have overcome lack of immunogenicity by immunizing *msh3*-null mice with a recombinant MSH3 fragment and by producing a panel of 10 monoclonal antibodies (mAbs). Two of the 10 antibodies showed no evidence of cross-reaction with other, more abundant proteins by western blot analysis and show strong nuclear-specific signal by immunocytochemistry. Although MSH3 can be expected to have a broadly similar localization to MSH2 in mice, only one study using immunohistochemistry reported MSH3-specific expression in mouse neuronal cells [Gonitel et al., 2008]. No experiment has determined the precise cellular localization of MSH3 in mouse cells. In this paper, we clearly demonstrate the specificity of two MSH3 generated antibodies. This allowed us to determine the localization of MSH3 within the nucleoplasm of both primary and transformed, human and mouse cell lines. Furthermore, we observed changes in the nuclear localization of MSH3 and its co-localization with PCNA under conditions of stress.

MATERIALS AND METHODS

MSH3 FUSION PROTEIN PREPARATION

Trx-MSH3 (Thioredoxin-MSH3). A PCR fragment containing 855 bp of the N-terminus of mouse MSH3 (amino acids 24 to 308 of NCBI sequence NP_034959) was cloned into the *BamH*I and *Hind*III sites of pET32a, which contains a thioredoxin sequence. *E. coli* competent cells BL21(DE3) were transformed and the expression of PCR fragment was induced by IPTG to give a 43.5 kD recombinant fusion protein (31.5 kD MSH3 with 12 kD thioredoxin). Cells were subsequently washed with TNE buffer and sonicated sequentially with TNE, 2M urea, 4M urea, 6M urea and 8M urea. The majority of the fusion protein was extracted in 4M urea fraction, which was purified by His-bind column chromatography.

GST-MSH3. A smaller PCR fragment containing 492 bp of the N-terminus of mouse MSH3 (amino acids 24 to 187 of NCBI sequence NP_034959) was cloned into the *BamH*I and *Sma*I sites of vector pGEX 2T. BL21(DE3) cells were transformed with the resultant construct (pGEX-2B1) and the culture induced with IPTG to give a 44 kD recombinant fusion protein (18 kD MSH3 with 26 kD GST tag). After incubation, cells were washed with TNE buffer and then sonicated sequentially with TNE, 2M urea, 4M urea, 6M urea and 8M urea. Fusion protein was extracted in the TNE and 2M urea fractions. Fusion protein in the TNE fraction was further purified by binding glutathione-Sepharose 4B beads and eluting with 10 mM glutathione.

HYBRIDOMA PRODUCTION

Recombinant MSH3 fusion proteins were used as immunogens for production of monoclonal antibodies using the hybridoma method [Nguyen and Morris, 2010]. Mice were either regular Balb/c strain or *msh3* knock-out mice (129/OLA/FVB/Bl/6) [de Wind et al., 1999]. The antibody titres in mouse sera were determined by ELISA prior to fusion. Antibody-producing B lymphocytes from spleen were fused with Sp2/0 myeloma cells and allowed to proliferate in ten 96 well plates. Culture media from wells were firstly screened by ELISA. Medium identified as positive were further screened by western blot and immunofluorescent staining of cells on coverslips. Hybridomas in wells were cloned by limiting dilution and the resultant colonies screened again. Cloning by limiting dilution was continued until all resultant colonies were positive and therefore monoclonal. Ig subclasses were determined using an isotyping kit (Zymed Labs Inc., San Francisco).

ELISA

ELISA plates were coated with 10 μg/ml recombinant antigen, washed with PBS, blocked and washed again with PBS prior to incubation with either mouse serum or hybridoma culture supernatant. Mouse sera were initially at a dilution of 1/50 in the first well, followed by seven serial dilutions down to 1/109,350. To screen hybridomas, culture medium was added to the ELISA plate at a dilution of 1/4. Following incubation with serum or culture supernatant, plates were washed and then incubated with 1/1000 rabbit anti-mouse HRP conjugate (Dako). Plates were again washed and color developed with either tetramethylbenzidine (TMB) or o-phenylenediamine dihydrochloride (OPD) substrates. The reaction was stopped with 3M H_2SO_4 and absorbance measured at 450 nm (for TMB) or 490 nm (for OPD).

SDS-POLYACRYLAMIDE GEL ELECTROPHORESIS AND WESTERN BLOTTING

Cultured cells were extracted in 125 mM Tris pH 6.8, 2% SDS, 5% 2-beta mercaptoethanol, 5% glycerol with protease inhibitors (Sigma P8340 plus 1 mM PMSF). Tissue samples (250 mg/ml) were extracted in: 50 mM Tris pH 6.8, 1% EDTA, 10% SDS, 5% beta mercaptoethanol, 10% glycerol with protease inhibitors. After the addition of bromophenol blue and after boiling, samples were subjected to SDS-PAGE using 10% polyacrylamide gels and transferred to

nitrocellulose membranes (Protan BA85, Whatman). After blocking non-specific sites with 5% skimmed milk protein, membranes were incubated with monoclonal antibody which was present in culture medium (1/25 dilution). Antibody reacting bands were visualized following development with peroxidase-labelled goat anti-mouse Ig and a chemiluminescent detection system (SuperSignal, Pierce).

EUKARYOTIC CELL CULTURE AND IMMUNOFLUORESCENT STAINING

Eukaryotic cells (C2C12, MEFs, HeLa and human skin fibroblasts) were grown in DMEM with 10% fetal bovine serum. To induce oxidative stress, C2C12 cultures were treated with either 1 mM ethanol or 1 mM hydrogen peroxide for 22 hours. For prolonged oxidative stress, C2C12 cells were cultured with 1 mM hydrogen peroxide for 4 days. For immunohistochemistry, cells on coverslips were fixed with 50:50 acetone-methanol and washed 4 times with PBS. Culture supernatants containing anti-MSH3 monoclonal antibodies were diluted 1:3 in PBS and incubated on coverslips for 1 hour at room temperature. For double labeling, cells were initially incubated with 4 μg/ml rabbit polyclonal anti-PCNA (SC-7907, Santa Cruz) for 1 hour, followed by washing and incubation with monoclonal anti-MSH3. Alternatively, cells were initially incubated with 1:200 Phospho-Histone H2A.X (Ser139) Rabbit mAb (Cell Signaling Technology; No:9718; New England Biolabs, Hitchin, UK) for 1 hour, followed by washing and incubation with 1:3 anti-MSH3 mouse mAb. Following washing, cells were then incubated with 5 μg/ml goat anti-mouse ALEXA 488 (Molecular Probes, Eugene, Oregon, USA) secondary antibody diluted in PBS containing 1% horse serum, 1% fetal bovine serum and 0.1% BSA, for 1 hour. For double label, 5 μg/ml goat anti-rabbit ALEXA 546 (Molecular Probes, Oregon, USA) was included within the secondary antibody mix. DAPI (diamidino phenylindole at 200 ng/ml) was added for the final 5 mins of incubation to counterstain nuclei before mounting in Hydromount (Merck).

Cells were examined and sequential confocal scans performed with a Leica TCS SP5 spectral confocal microscope (Leica Microsystems, Milton Keynes, UK). Imaging lasers used were a Blue Diode 405 nm laser for DAPI, an Argon 488 nm laser for ALEXA 488 and a Helium/Neon 543 nm laser for ALEXA 546.

EPITOPE MAPPING

Epitope mapping using phage-displayed random peptide libraries in filamentous phage was performed as previously described [Pereboev and Morris, 1996], using a modification of an earlier method [Smith et al., 1992]. Monoclonal antibodies were diluted 1:50 with Tris-buffered saline (TBS) and immobilised onto sterile 35 mm Petri dishes coated directly with 1 ml of 1:200 dilution of rabbit-anti-[mouse Ig] in TBS (Dako, Denmark). Biopanning was performed using a 15-mer peptide library in phage f88-4 maintained in the K91Kan strain of *Escherichia coli*, generously supplied by G.P. Smith (University of Missouri). Any remaining binding sites on the dishes were blocked using 4% BSA in sterile TBS. The phage library was pre-incubated in dishes coated with the rabbit anti-mouse antibodies alone to ensure any binding was specific for the MSH3 mAbs. Following the first round of biopanning, the bound phage were eluted and amplified by infection of K91Kan *E. coli* cells. Three rounds of biopanning were performed. Colonies of the phage infected cells after the third round were grown on nitrocellulose membrane and screened with MSH3 mAbs to reveal positive clones. Purified phage DNA was sequenced using primer: 5′-AGTAGCA-GAAGCCTGAAGA-3′.

RESULTS

MSH3 MONOCLONAL ANTIBODY PRODUCTION

In a first attempt to create efficient MSH3 antibodies, sera from three Balb/c mice immunized with GST-MSH3 (amino acids 24 to 187 of mouse MSH3 with a GST tag) were obtained and gave a strong reaction against the GST tag by ELISA, but only a weak reaction against the MSH3 component. Similarly, serum from three Balb/c mice immunized with a larger fusion protein, Trx-MSH3 (amino acids 24 to 308 of mouse MSH3 with a thioredoxin tag) gave a strong reaction with thioredoxin but only a weak reaction with MSH3. Hybridoma fusions performed with spleens from such mice failed to produce MSH3-reactive clones.

We then decided to immunize *msh3*-deficient mice (*msh3* −/−) to improve the reaction with MSH3. When the Trx-MSH3 fusion protein was used to immunize three *msh3* −/− mice, the sera showed strong reaction against MSH3, as determined by coating the ELISA plate with GST-MSH3 (Fig. 1). The response to the MSH3 component of the fusion protein was at least 10-fold greater in the *msh3* knock-out mice compared with the wild-type mice (Fig. 1).

A fusion between Sp2/0 myeloma cells and spleen cells from a Trx-MSH3-immunized *msh3*-null mouse was screened by ELISA and 111 out of 960 wells gave a positive reaction with Trx-MSH3, but not with Trx alone. Of these, 88 of the strongest were further screened by western blot with Trx-MSH3 and 49 gave a strong reaction. Of these 49, 28 of the strongest were tested for reaction with endogenous protein by western blot (wild-type and *msh3*−/− mouse testis extracts) and for immunofluorescence staining of

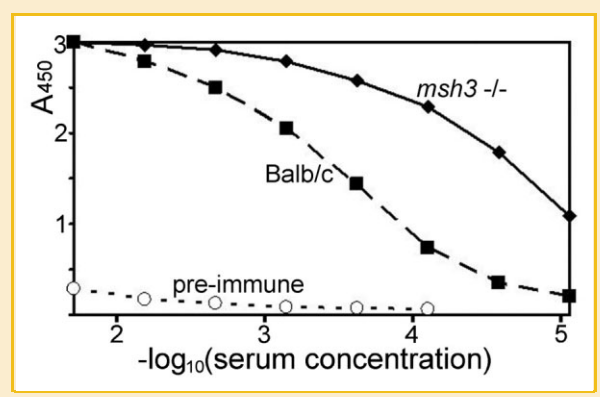

Fig. 1. ELISA screen of mouse sera following immunization with Trx-MSH3 antigen. Balb/c (wild-type) mice and *msh3* −/− mice were immunized with Trx-MSH3 (MSH3 amino acids 24 to 308 with a thioredoxin tag). ELISA plates were coated with GST-MSH3, to detect antibodies in sera which bind the MSH3 component of the immunogen and not those antibodies reacting with thioredoxin. Serial tripling dilutions were performed on sera from mice which were pre-immune (open circle, small dashed line); Balb/c immunized with Trx-MSH3 (solid square, large dashed line) and *msh3* −/− mice immunized with Trx-MSH3 (solid diamond, solid line).

TABLE I. Characterization of Anti-MSH3 Monoclonal Antibodies

Monoclonal antibody			Mouse		Human	
Name	Clone	Isotype	WB	IMF	WB	IMF
MSH3MAB1	1F6	IgG1	+++	++	–	–
MSH3MAB2	2F11	IgG1	+++	++	–	–
MSH3MAB3	5A5	IgG1	+++	+	+++	++
MSH3MAB4	8E6	IgG1	++	+	+++	+
MSH3MAB5	7H12	IgG1	++	–	–	–
MSH3MAB6	5D6	IgG1	++	–	–	–
MSH3MAB7	9E11	IgG1	++	–	–	–
MSH3MAB8	2A9	IgG1	++	–	–	–
MSH3MAB9	7A10	IgG1	++	–	–	–
MSH3MAB10	9B11	IgG1	+	–	–	–

WB = western blot. "+++, ++ or +" indicate the intensity of the band of correct size (123 kD). Mouse WB was done with tissue (testis), MEFs and C2C12 and human WB with HeLa. With the mouse tissue and MEFs, a band of correct size was present on the wild-type blot and was absent from the *msh3*-knock out blot. IMF = Immunofluorescence stain. "++ or +" indicates the intensity of a general nuclear stain. This general nuclear stain was present in wild-type MEFs but absent from *msh3*-knockout MEFs. "–" indicates that the IMF did not show a general nuclear staining pattern and these images were either negative, or, the mAbs gave staining patterns which were speckle-like (MSH3MAB5) or with large nuclear structures (MSH3MAB6, 7, 8 and 9), present in both wild-type and knockout MEFs. Human IMF data from HeLa and cultured skin fibroblasts.

cultured mouse C2C12 myoblasts. This screen identified mAbs which stained mouse nuclei and also gave a western blot band of predicted size, absent from *msh3*-null mice. After cloning by limiting dilution, ten hybridomas were produced (Table I).

CHARACTERIZATION AND SPECIFICITY OF ANTI- MSH3 MABS

On western blots of mouse C2C12 myogenic cell extracts, all ten mAbs gave a double band close to the expected size of 123 kD (Fig. 2A and Table I). Six of these mAbs also stained a likely cross-reacting protein of about 110 kD. Two mAbs recognised human MSH3 on western blots of HeLa extracts (Fig. 2B), and these also showed the strongest cross-reaction with the mouse 110kD band (Fig. 2A). All 10 mAbs stained a 123kD MSH3 band in mouse testis tissue extracts, which was absent from *msh3*–/– mouse extracts. This is shown in Figure 3 for the four strongest mAbs, together with MBNL1 as an equal loading control. The cross-reactive band stained by MSH3MAB3 and 4 was present in *msh3*–/– mice (Fig. 3).

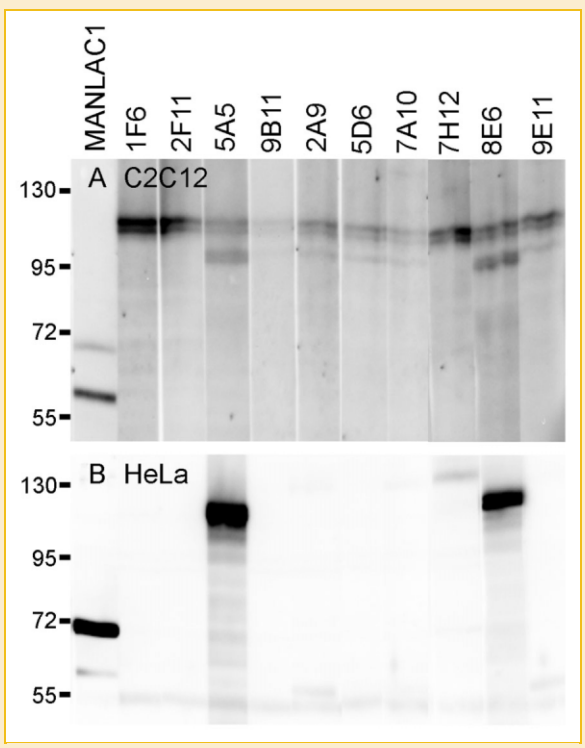

Fig. 2. The mAbs detect an MSH3 band of expected size on western blots. Western blot of C2C12 mouse cell extract (A) and HeLa extract (B) were developed with the anti-MSH3 panel of 10 mAbs (see Table I for clone numbers). (A) Major bands with the C2C12 extract were at the expected size of MSH3 (123 kD), with some smaller bands also evident for 6 of the mAbs. (B) Two of the mAbs also recognised human MSH3. The control mAb is MANLAC1 (1:100 dilution) which recognises lamin A/C (71kD and 66kD).

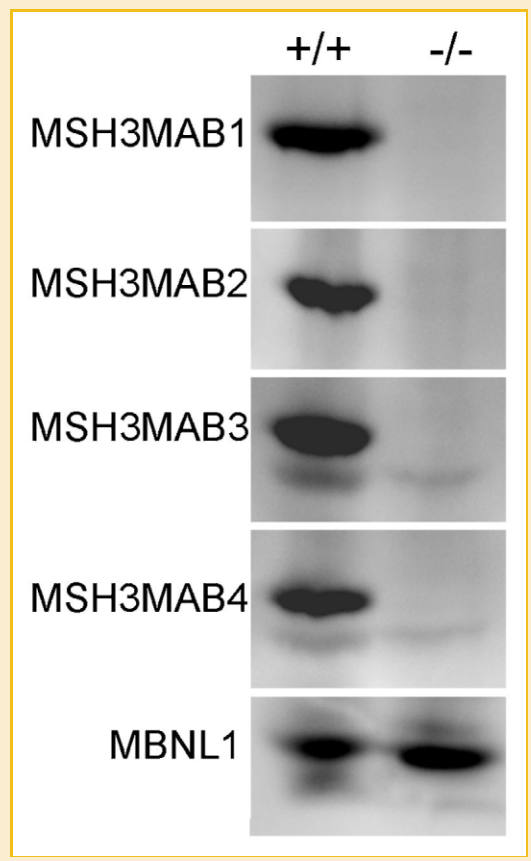

Fig. 3. Specificity of the mAbs for mouse MSH3. Western blot of testis tissue extract from wild-type (+/+) and *msh3*-null (–/–) mice were developed with 4 of the strongest anti-MSH3 mAbs. The 4 mAbs gave a band of 123 kD in wild-type which was completely absent from the *msh3*-null extract. Two of the mAbs also had cross-reacting, lower molecular weight bands with both extracts. Shown as a loading control was mAb MB1a against MBNL1 which gave 42 kD bands with both extracts.

We then tested the MSH3 antibodies by immunofluorescence microscopy in C2C12 cells and wild-type or *msh3* −/− mouse embryonic fibroblasts (MEFs). Four of them showed nuclear staining in wild-type MEFs that was absent from *msh3*−/− MEFs. Two of the mAbs, MSH3MAB1 and 2, gave predominantly nuclear staining in wild-type MEFs (Fig. 4BE). MSH3MAB3 and 4 showed stronger cytoplasmic staining, present in both wild-type and *msh3* −/− cells (Fig. 4HIKL) and the minor band on blots (Fig. 3) may be responsible for this cytoplasmic cross-reaction. The intensity of nuclear staining was variable in MEFs, possibly reflecting the heterogeneity of these cells, but it was stronger and more uniform in mouse C2C12 myoblasts (Fig. 4ADGJ).

The hybridoma cloning process effectively removed the cross-reactions typical of anti-MSH3 antisera. The immune mouse antiserum recognised numerous structures in the nuclei and in the cytoplasm of both wild-type and knockout cells, indicating that much of the immune response was not MSH3-specific (Fig. 5A). MSH3MAB6 showed some nuclear staining that was only present in the wild-type cells, but this mAb also stained large nuclear structures in both wild-type and knockout MEFs (Fig. 5B). mAb MSH3MAB1 had a nucleoplasmic localization in wild-type cells which was completely absent from the knock-out cells, thus showing the authentic distribution of MSH3 (Fig. 5C). MSH3MAB3 and 4 stained the nuclei of HeLa cells and human skin fibroblasts, whereas the other mAbs did not (Fig. 6). However, MSH3MAB4 also recognised additional large nuclear structures in the human cells (Fig. 6GH), presumably as a result of cross-reaction. The cytoplasmic cross-reaction that MSH3MAB3 and 4 display in mouse cells was much less apparent in human cells. The results show that MSH3MAB1 and 2 are specific and best for mouse MSH3, while MSH3MAB3 is the best choice for human MSH3 detection.

Epitope mapping using a phage-displayed peptide library (Fig. 7) showed that MSH3MAB1, 2 and 5 bind to the same region of the mouse MSH3 protein (amino acids 33 to 39) which is less highly-conserved (3 out of the 7 amino-acids in the epitope different

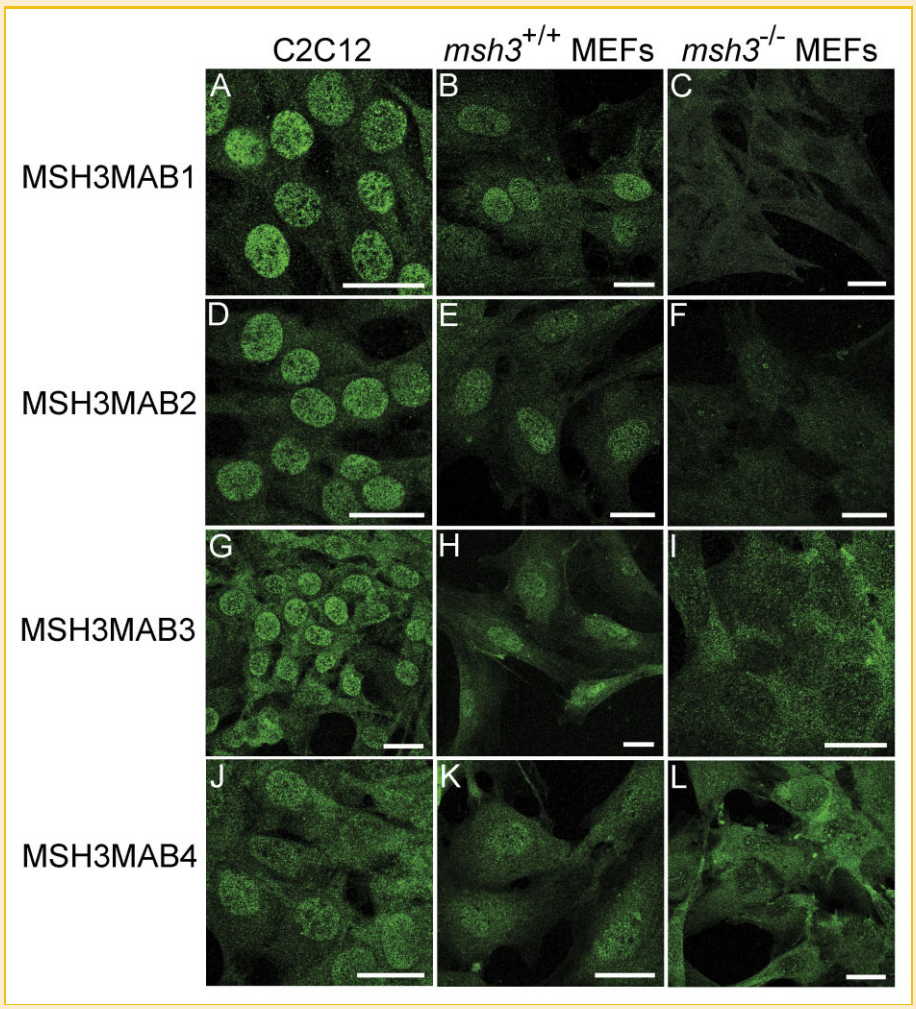

Fig. 4. Immunolocalization of MSH3 in mouse cells. MSH3MAB1 and 2 gave only nuclear staining in C2C12 (A,D) and wild-type MEFS (B,E), whilst *msh3*-null MEFs were completely blank (C,F). MSH3MAB3 and 4 also localized to nuclei but gave additional cytoplasmic staining in C2C12 (G,J) and wild-type MEFs (H,K). With *msh3*-null MEFs, nuclei were not stained, but cytoplasmic localization occurred with the latter two mAbs (I,L). Bar = 25 μm. [Color figure can be viewed in the online issue, which is available at wileyonlinelibrary.com]

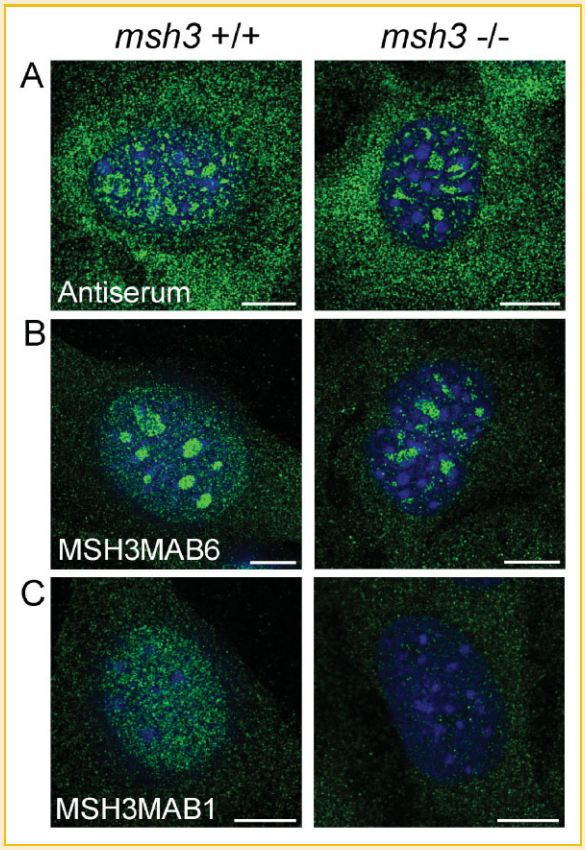

Fig. 5. Different immunolocalization patterns in wild-type (+/+) and *msh3*-null (−/−) MEFs. Immune mouse antiserum recognises numerous structures in both cell types. MSH3MAB6 showed some nuclear staining that was only present in wild-type cells, but it also stained large nuclear structures in both cell types. In wild-type cells, MSH3MAB1 showed a nucleoplasmic distribution, which was largely absent from areas which were stained intensely by DAPI. As shown previously, MSH3MAB1 does not localize to *msh3*-null MEFs. Bar = 10 μm. [Color figure can be viewed in the online issue, which is available at wileyonlinelibrary.com]

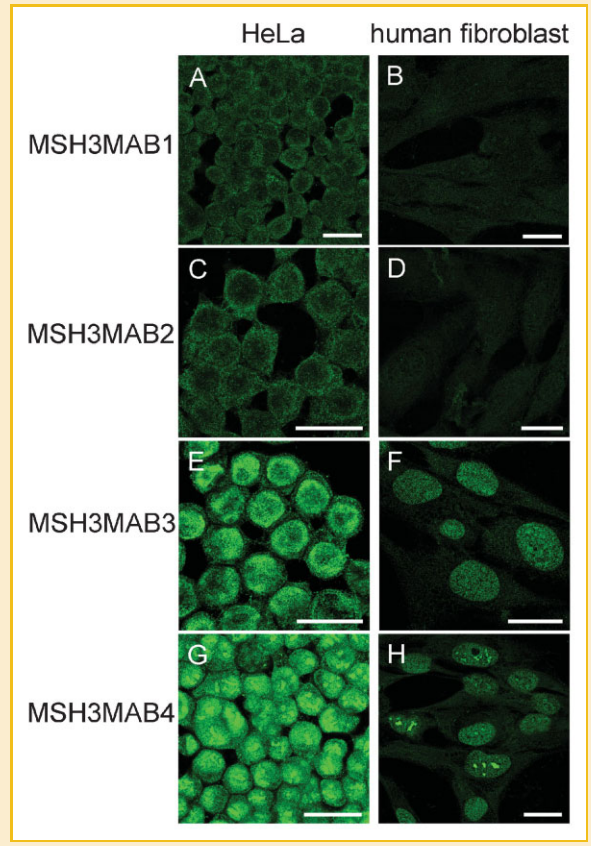

Fig. 6. Immunolocalization of MSH3 in human cells. MSH3MAB1 and 2 did not stain structures in HeLa (A,C) or in human skin fibroblasts (B,D). Whereas, MSH3MAB3 and 4 showed nuclear localization in HeLa (E,G) and fibroblasts (F,H), with MSH3MAB4 recognising some additional nuclear structures. Bar = 25 μm. [Color figure can be viewed in the online issue, which is available at wileyonlinelibrary.com]

between man and mouse), thus explaining their specificity for mouse MSH3. In contrast, all amino-acids in the epitope for MSH3MAB3 and 4 are identical in human and mouse proteins (amino acids 187 to 194 of mouse MSH3, accession P13705).

CO-LOCALIZATION OF MOUSE MSH3 AND PCNA IN THE NUCLEUS UNDER OXIDATIVE STRESS

We have demonstrated the specificity of the localization of MSH3MAB1 and 2 by showing the absence of immunostaining in a cell line from the *msh3*−/− mouse (Fig. 4CF and Fig. 5C). We have shown that MSH3 is a nuclear protein with a finely-granular nucleoplasmic distribution (Figs. 4 and 5) which is largely absent from areas of DAPI-intense heterochromatin (Fig. 5C).

In order to investigate the localization of MSH3 after oxidative stress, we used our new antibodies to determine its nuclear distribution along with the distribution of PCNA, which is known to interact with MSH3 during DNA damage repair. Both ethanol and hydrogen peroxide (H_2O_2) cause oxidative stress in cells by the production of free radicals (reactive oxygen species) [Lieber, 1997].

Using MSH3MAB1, we studied MSH3 localization in untreated control C2C12 cells and in C2C12 cells treated with either 1 mM ethanol or 1 mM H_2O_2 for 22 hours. In untreated cells, MSH3 was distributed homogeneously throughout the nucleoplasm and not especially co-localized with PCNA (Fig. 8A). In approximately 11% (46 of a total of 404) of ethanol-treated cells and 4% (31 of a total of 691) of H_2O_2-treated cells, MSH3 and PCNA appeared to co-localize in nuclear bodies that were not seen in control cell cultures (Fig. 8BC). The phosphorylation of Ser139 in the C-terminal tail of Histone H2A.X is a common signalling marker of DNA damage response. Double labels were performed to determine whether there was any association between phospho-H2A.X (also known as γ-H2AX) and MSH3. The distribution of MSH3 in Control (Fig. 8D) and C2C12 cells treated with hydrogen peroxide for 22 hours (Fig. 8E) was similar to that seen previously (Fig. 8A and C). Phospho-H2A.X was not detected in these cells (Fig. 8DE). However, with prolonged (4 day) exposure to hydrogen peroxide, nuclear staining for phospho-H2A.X was observed in a low number of cells. Co-localization of MSH3 and phospho-H2A.X was observed in nuclear bodies in 2.6% (6 of a total of 229) of the cells treated with hydrogen peroxide for 4 days (Fig. 8F).

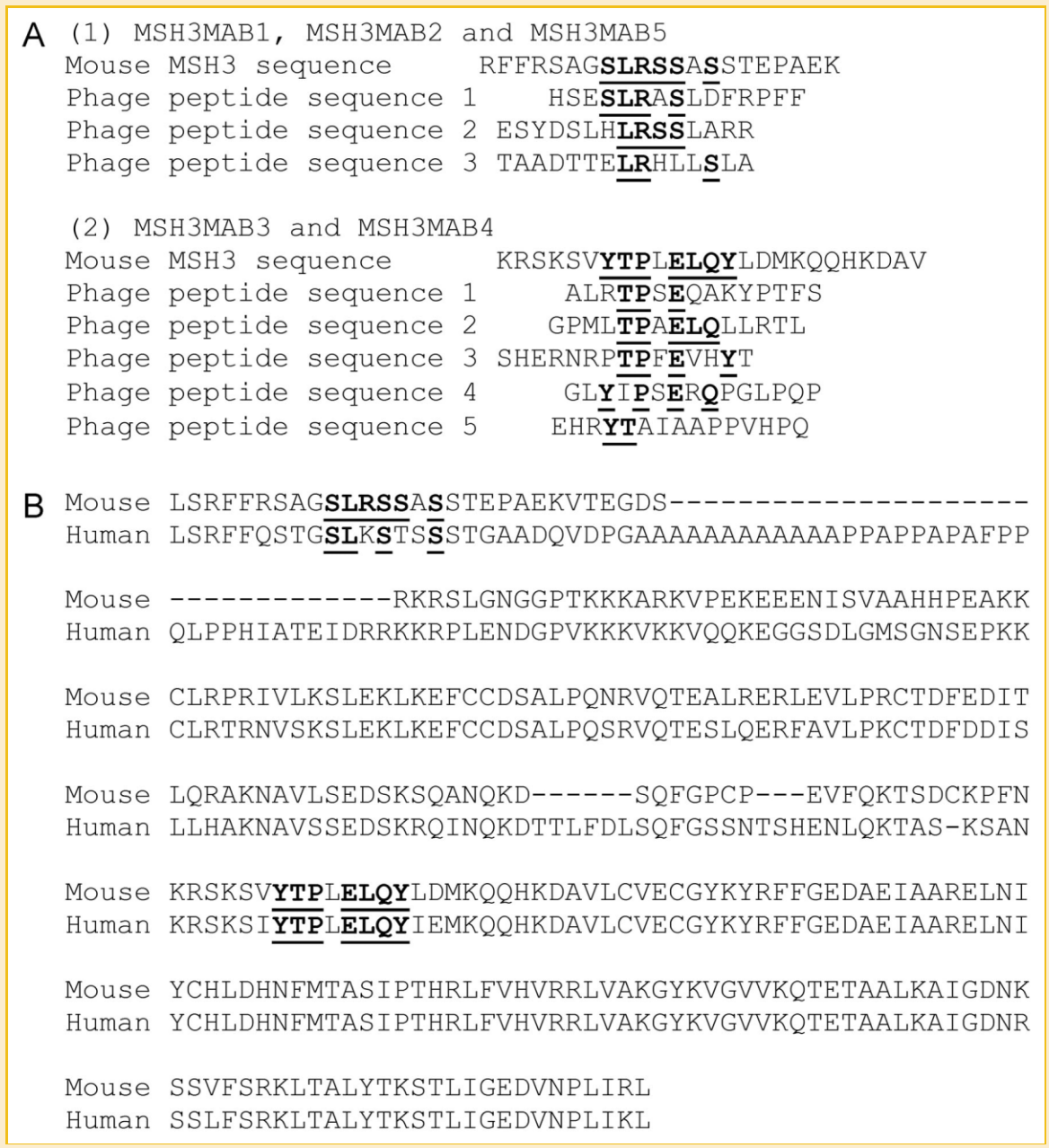

Fig. 7. Epitope mapping using a phage-display peptide library. (A) For the two epitopes identified, we show the names of the mAbs that recognise the epitope, the sequence of mouse msh3 that contains the epitope and the sequences of the 15-mer peptides pulled out of the library. Matching amino acids in the mouse sequence and the peptides are aligned and shown in bold and underlined. (B) Amino acids 24 to 308 of mouse MSH3 (Accession: P13705; upper line) aligned with the corresponding sequence of human MSH3 (lower line). This mouse sequence was the immunogen for the mAb production. Amino acids identified in the two regions of antibody binding are shown bold and underlined.

DISCUSSION

MSH3 studies in mice have suffered due to the lack of specific antibodies. Most antibodies available so far usually give strong background in western blot analysis and/or in immunofluorescence studies. Here, we report for the first time in mice, MSH3 cellular localization using antibodies raised specifically against the mouse protein. Production of mouse mAbs against mouse MSH3 was entirely dependent on the use of MSH3-deficient mice for immunization, because mouse MSH3 is non-immunogenic in wild-type mice. Use of knockout mice to overcome immune tolerance to endogenous proteins has been used before [Castrop et al., 1995; Roes et al., 1995; Rogers et al., 2006]. *E.g.*, Castrop et al. [1995] have developed a nuclear T cell protein TCF-1 antibody by immunization of *Tcf-1*-deficient mice. Together with our results, this suggests that knockout mice can be essential to produce murine monoclonal antibodies. Two of the new antibodies (MSH3MAB1 and MSH3MAB2) showed in western blot a clean and strong signal for MSH3 that was absent from the *msh3*−/− control tissue. MSH3MAB2 has been successfully used to investigate the impact

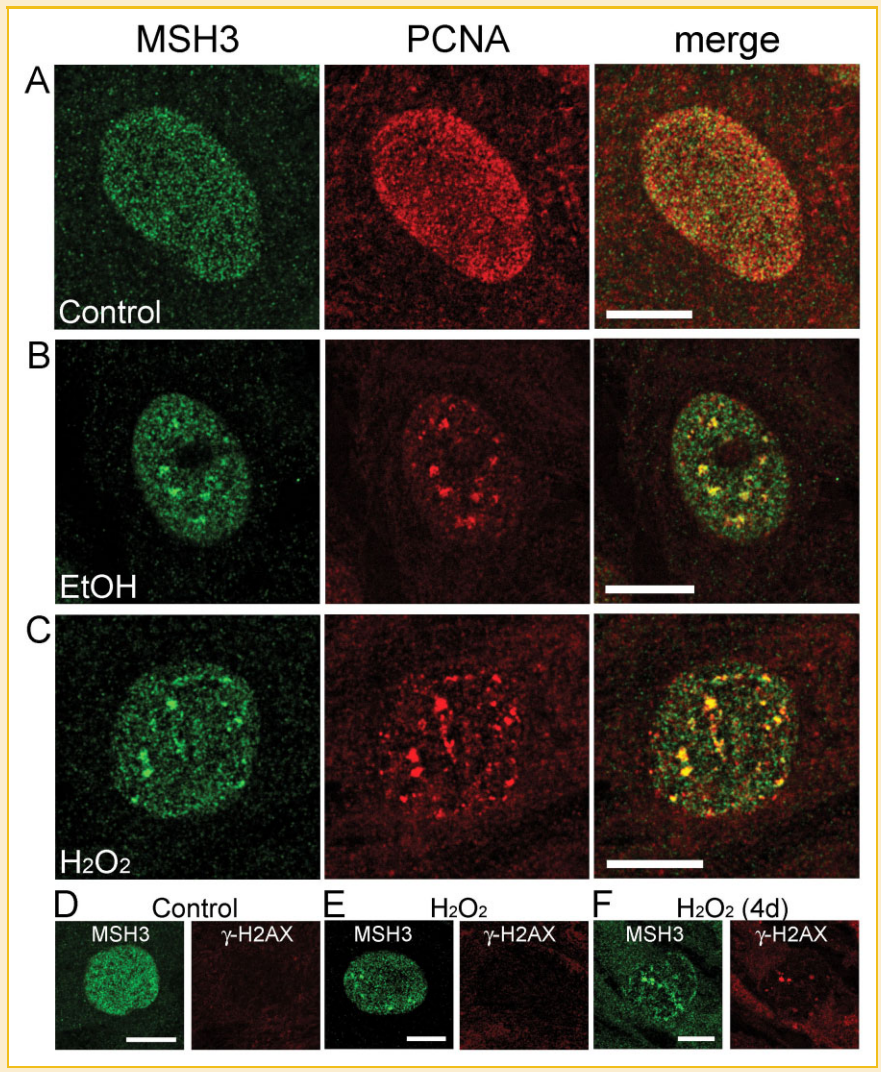

Fig. 8. Colocalization of MSH3 and PCNA under conditions of oxidative stress. Immunolocalization of MSH3 (MSH3MAB1), PCNA and the merged image of MSH3 + PCNA + DAPI (right panel) in C2C12 cells. Images are shown for untreated control culture (A) and for cultures in which oxidative stress had been induced by ethanol (B) or hydrogen peroxide (C) for 22 hours. Conversely, phospho-H2A.X (γ-H2AX) was absent from control cultures (D) and from those treated with hydrogen peroxide for 22 hours (E). After 4 days of treatment with hydrogen peroxide, phospho-H2A.X was colocalized with nuclear spots of MSH3 in a low number of cells (F). Bar = 10 μm. [Color figure can be viewed in the online issue, which is available at wileyonlinelibrary.com]

of MSH3 expression levels on CTG repeat instability in various transgenic mouse tissues [Tomé et al., 2009].

In this study, we focused on the localization of MSH3 within the cell. We found that MSH3 had a finely-granular distribution throughout the nucleoplasm; the specific antibodies MSH3MAB1 and MSH3MAB2 showed a clear nuclear staining, but no cytoplasmic staining (except a background seen also in *msh3* −/− cells). This nuclear staining disappeared in *msh3* −/− cells confirming the specific nuclear localization of MSH3. MSH3MAB3 and MSH3MAB4 showed a non-specific band of lower Mr on western blot of mouse cells and also showed cytoplasmic staining in both wild-type and *msh3*−/− cells. There are few previous reports of immunohistochemical localization in mice. In the only published study of mouse tissues, Gonitel et al. [2008] used a polyclonal goat antiserum against human MSH3 (Santa Cruz Biotechnology) for immunohistochemical detection of MSH3 in neuronal cells in sections of brain striatum from Huntington's disease model mice and wild-type mice [Gonitel et al., 2008]. This antiserum showed a more granular distribution of MSH3 in both nucleus and cytoplasm, compared with the mAbs in our present study, but the possibility that some of the immunofluorescence (including that in the cytoplasm) could be due to cross-reaction with non-MSH3 proteins was not examined. Our present studies have shown that MSH3 levels can vary between cells in a heterogeneous population of MEFs, possibly due to variation between different cell types. On another hand, MSH3 protein levels may vary during cell cycle in asynchronous cell cultures of MEFs [Schilling and Farnham, 1995].

Laser micro-irradiation of human cells have shown that MMR proteins were recruited to the sites of DNA damage and that MSH3 accumulated via its PCNA interacting domain [Hong et al., 2008].

Furthermore, MutSβ was also recruited to UV-irradiated sites in nucleotide-excision-repair- and PCNA-dependent manners. Thus, MMR proteins, including MSH3, are directly involved in DNA damage repair. Another study in human cells reported that non-cytotoxic levels of H_2O_2 inactivated both single-base mismatch and loop repair activities of the MMR system in a dose-dependent fashion [Chang et al., 2002]. However, the level of MSH3 proteins was not determined and was below the detection level. In our study, we clearly observed that MSH3 is a nuclear protein distributed with a fine granularity in the entire nucleus. Under condition of oxidative stress, the localization of MSH3 changed and accumulated in denser nuclear bodies with PCNA. This observation, consistent with the established direct interaction between these two proteins, strengthens the role of MSH3 and PCNA interaction in DNA damage response.

Oxidative stress induced by hydrogen peroxide and other reactive oxygen species can damage multiple functional pathways in cells and can lead to different types of DNA lesions. A common base modification generated by reactive oxygen species is the conversion of guanine to 7,8-dihydro-8-oxoguanine (8-oxoG), with the subsequent misincorporation of adenine opposite 8-oxoG, that can lead to G-T transversions in the DNA [Chatgilialoglu and O'Neill, 2001; Valko et al., 2004]. In addition to mutations in the base sequence, hydrogen peroxide can also lead to single and double strand breaks [Valko et al., 2004; Zhang et al., 2009]. Hydrogen peroxide has also been shown to induce topoisomerase 1 (TOP1)-DNA cross-links on oxidative DNA lesions to form TOP1-DNA cleavage complexes [Daroui et al., 2004]. DNA damage responses are complex and several pathways have been elucidated. Their roles include the detection of damaged DNA, activation of repair, delay of the cell cycle and activation of apoptosis [Harper and Elledge, 2007; Jackson and Bartek, 2009]. Histone H2A is one of four core histone proteins that make up the nucleosome. One of the most widely studied markers of DNA damage in higher eukaryotes is the phosphorylation of Serine-139 of H2A.X. After DNA double-strand breaks, serine/threonine protein kinases, such as ataxia telangiectasia mutated (ATM), ataxia telangiectasia and Rad3 related (ATR) and DNA dependent protein kinase (DNA-PK) are recruited to the lesion [Lee and Paull, 2005; Berkovich et al., 2007] and phosphorylate the histone variant H2A.X at Ser139 residue in mouse and human cells [Bonner et al., 2008]. Phospho-H2A.X (γ-H2AX) is one of the first proteins to accumulate at double strand breaks and is required for the retention of several DNA damage response proteins at DNA damage foci. The repair proteins present at the damage site may vary with different conditions and between different cell types. Phospho-H2A.X has been implicated in the DNA damage response involving non-homologous end joining and homologous recombination repair pathways and has been shown to colocalize with several DNA repair proteins such as Rad50, Rad51, Nbs1, MDC1 yRad9/53BP1 and BRCA1 [cited by Altaf et al., 2009].

Unlike the colocalization between MSH3 and PCNA that was observed in cells which had been treated with hydrogen peroxide for 22 hours, phospho-H2A.X was not detected at this time. However, after prolonged oxidative stress (4 days exposure to hydrogen peroxide), phospho-H2A.X was detected and found to co-localize with MSH3 in nuclear bodies in a low number of cells. Mismatch repair proteins have been implicated in the cellular DNA damage response and MSH3 is recruited to DNA damage sites in a PCNA dependent manner [Hong et al., 2008]. Using a photosensitizer and laser irradiation to induce DNA damage which included double strand breaks, Hong et al. [2008] showed colocalization between MSH3 and phospho-H2A.X at the laser-irradiated sites. Our results indicate that DNA damage induced by hydrogen peroxide is time dependent. With 22 hours exposure to hydrogen peroxide, PCNA and MSH3 are recruited to nuclear foci, which are probably DNA damage sites that do not contain double strand breaks. Exposure to hydrogen peroxide for 4 days leads to a type of DNA damage that induces phospho-H2A.X and its recruitment to MSH3 foci.

In conclusion, we have developed mouse monoclonal antibodies specific for mouse and human MSH3. These mAbs will be valuable tools to study MSH3 localization, expression and role in various pathways such as DNA repair, DNA damage response, cancer, and trinucleotide repeat instability, especially in mouse models.

ACKNOWLEDGMENTS

This study was supported by grants from Association Francaise contre les Myopathies (IH and GG), the RJAH Institute of Orthopaedics and by Translational Infrastructure Grants for the MDA Monoclonal Antibody Resource from the Muscular Dystrophy Association (GEM). Work in the Gourdon lab was also supported by the Institut National de la Santé et de la Recherche Médicale, the Agence National de la Recherche and a PhD grant from the Ministère Français de la Recherche et de la Technologie (ST). We thank Pinochet Tchassie for technical assistance and George P. Smith lab (Division of Biological Sciences, University of Missouri) for phage-displayed peptide libraries.

REFERENCES

Altaf M, Auger A, Covic M, Côté J. 2009. Connection between histone H2A variants and chromatin remodeling complexes. Biochem Cell Biol 87:35–50.

Berkovich E, Monnat RJ Jr, Kastan MB. 2007. Roles of ATM and NBS1 in chromatin structure modulation and DNA double-strand break repair. Nat Cell Biol 9:683–690.

Bonner WM, Redon CE, Dickey JS, Nakamura AJ, Sedelnikova OA, Solier S, Pommier Y. 2008. GammaH2AX and cancer. Nat Rev Cancer 8:957–967.

Castrop J, Verbeek S, Hofhuis F, Clevers H. 1995. Circumvention of tolerance for the nuclear T cell protein TCF-1 by immunization of TCF-1 knock-out mice. Immunobiology 193:281–287.

Chang CL, Marra G, Chauhan DP, Ha HT, Chang DK, Ricciardiello L, Randolph A, Carethers JM, Boland CR. 2002. Oxidative stress inactivates the human DNA mismatch repair system. Am J Physiol Cell Physiol 283:C148–154.

Chao EC, Lipkin SM. 2006. Molecular models for the tissue specificity of DNA mismatch repair-deficient carcinogenesis. Nucleic Acids Res 34:840–852.

Chatgilialoglu C, O'Neill P. 2001. Free radicals associated with DNA damage. Exp Gerontol 36:1459–1471.

Clark AB, Valle F, Drotschmann K, Gary RK, Kunkel TA. 2000. Functional interaction of proliferating cell nuclear antigen with MSH2-MSH6 and MSH2-MSH3 complexes. J Biol Chem 275:36498–36501.

Daroui P, Desai SD, Li TK, Liu AA, Liu LF. 2004. Hydrogen peroxide induces topoisomerase I-mediated DNA damage and cell death. J Biol Chem 279: 14587–14594.

de Wind N, Dekker M, Claij N, Jansen L, van Klink Y, Radman M, Riggins G, van der Valk M, van't Wout K, te Riele H. 1999. HNPCC-like cancer predisposition in mice through simultaneous loss of Msh3 and Msh6 mismatch-repair protein functions. Nat Genet 23:359–362.

Dragileva E, Hendricks A, Teed A, Gillis T, Lopez ET, Friedberg EC, Kucherlapati R, Edelmann W, Lunetta KL, MacDonald ME, Wheeler VC. 2009. Intergenerational and striatal CAG repeat instability in Huntington's disease knock-in mice involve different DNA repair genes. Neurobiol Dis 33:37–47.

Foiry L, Dong L, Savouret C, Hubert L, te Riele H, Junien C, Gourdon G. 2006. Msh3 is a limiting factor in the formation of intergenerational CTG expansions in DM1 transgenic mice. Hum Genet 119:520–526.

Gonitel R, Moffitt H, Sathasivam K, Woodman B, Detloff PJ, Faull RLM, Bates GP. 2008. DNA instability in postmitotic neurons. PNAS 105:3467–3472.

Harper JW, Elledge SJ. 2007. The DNA damage response: Ten years after. Mol Cell 28:739–745.

Hirata H, Hinoda Y, Kawamoto K, Kikuno N, Suehiro Y, Okayama N, Tanaka Y, Dahiya R. 2008. Mismatch repair gene MSH3 polymorphism is associated with the risk of sporadic prostate cancer. J Urol 179:2020–2024.

Hong Z, Jiang J, Hashiguchi K, Hoshi M, Lan L, Yasui A. 2008. Recruitment of mismatch repair proteins to the site of DNA damage in human cells. J Cell Sci 121:3146–3154.

Jackson SP, Bartek J. 2009. The DNA-damage response in human biology and disease. Nature 461:1071–1078.

Jiricny J. 2006. The multifaceted mismatch-repair system. Nat Rev Mol Cell Biol 7:335–346.

Lee JH, Paull TT. 2005. ATM activation by DNA double-strand breaks through the Mre11-Rad50-Nbs1 complex. Science 308:551–554.

Lieber CS. 1997. Role of oxidative stress and antioxidant therapy in alcoholic and nonalcoholic liver diseases. Adv Pharmacol 38:601–628.

Manley K, Shirley TL, Flaherty L, Messer A. 1999. Msh2 deficiency prevents in vivo somatic instability of the CAG repeat in Huntington disease transgenic mice. Nat Genet 23:471–473.

Nguyen TM, Morris GE. 2010. A rapid method for generating large numbers of high-affinity monoclonal antibodies from a single mouse. In: walker JM, editor. The Protein Protocols Handbook 3rd Edition. Totowa NJ: Humana Press. p 1961–1974.

Owen BA, Yang Z, Lai M, Gajec M, Badger JD 2nd, Hayes JJ, Edelmann W, Kucherlapati R, Wilson TM, McMurray CT. 2005. (CAG)(n)-hairpin DNA binds to Msh2-Msh3 and changes properties of mismatch recognition. Nat Struct Mol Biol 12:663–670.

Pearson CE, Nichol Edamura K, Cleary JD. 2005. Repeat instability: mechanisms of dynamic mutations. Nat Rev Genet 6:729–742.

Pereboev A, Morris GE. 1996. Reiterative screening of phage-display peptide libraries with antibodies. Methods Mol Biol 66:195–206.

Plaschke J, Krüger S, Jeske B, Theissig F, Kreuz FR, Pistorius S, Saeger HD, Iaccarino I, Marra G, Schackert HK. 2004. Loss of MSH3 protein expression is frequent in MLH1-deficient colorectal cancer and is associated with disease progression. Cancer Res 64:864–870.

Roes J, Müller W, Rajewsky K. 1995. Mouse anti-mouse IgD monoclonal antibodies generated in IgD-deficient mice. J Immunol Methods 183:231–237.

Rogers ML, Atmosukarto I, Berhanu DA, Matusica D, Macardle P, Rush RA. 2006. Functional monoclonal antibodies to p75 neurotrophin receptor raised in knockout mice. J Neurosci Methods 158:109–120.

Savouret C, Brisson E, Essers J, Kanaar R, Pastink A, te Riele H, Junien C, Gourdon G. 2003. CTG repeat instability and size variation timing in DNA repair-deficient mice. EMBO J 22:2264–2273.

Schilling LJ, Farnham PJ. 1995. The bidirectionally transcribed dihydrofolate reductase and rep-3a promoters are growth regulated by distinct mechanisms. Cell Growth Differ 6:541–548.

Smith MC, Ingham CJ, Owen CE, Wood NT. 1992. Gene expression in the Streptomyces temperate phage phi C31. Gene 115:43–48.

Stojic L, Brun R, Jiricny J. 2004. Mismatch repair and DNA damage signalling. DNA Repair (Amst) 3:1091–1101.

Tomé S, Holt I, Edelmann W, Morris GE, Munnich A, Pearson CE, Gourdon G. 2009. MSH2 ATPase domain mutation affects CTG*CAG repeat instability in transgenic mice. PLoS Genet 5:e1000482.

Valko M, Izakovic M, Mazur M, Rhodes CJ, Telser J. 2004. Role of oxygen radicals in DNA damage and cancer incidence. Mol Cell Biochem 266:37–56.

van den Broek WJ, Nelen MR, Wansink DG, Coerwinkel MM, te Riele H, Groenen PJ, Wieringa B. 2002. Somatic expansion behaviour of the (CTG)n repeat in myotonic dystrophy knock-in mice is differentially affected by Msh3 and Msh6 mismatch-repair proteins. Hum Mol Genet 11:191–198.

Wheeler VC, Lebel LA, Vrbanac V, Teed A, te Riele H, MacDonald ME. 2003. Mismatch repair gene Msh2 modifies the timing of early disease in Hdh(Q111) striatum. Hum Mol Genet 12:273–281.

Zhang R, Kang KA, Piao MJ, Ko DO, Wang ZH, Chang WY, You HJ, Lee IK, Kim BJ, Kang SS, Hyun JW. 2009. Preventive Effect of 7,8-Dihydroxyflavone against Oxidative Stress Induced Genotoxicity. Biol Pharm Bull 32:166–171.

Zhao J, Jain A, Iyer RR, Modrich PL, Vasquez KM. 2009. Mismatch repair and nucleotide excision repair proteins cooperate in the recognition of DNA interstrand crosslinks. Nucleic Acids Res 37:4420–4429.